HIGH PERFORMANCE SWING VELOCITY TRACKING CONTROL OF HYDRAULIC EXCAVATORS *

Bin Yao +, Jiao Zhang ++, Douglas Koehler ++, John Litherland ++

+ School of Mechanical Engineering
Purdue University
West Lafayette, IN 47907
byao@ecn.purdue.edu

++ Advanced Hydraulics Group, Caterpillar Inc.
Joliet, Illinois 60434-0504

Abstract

One of the issues in the swing motion control of an industrial hydraulic excavator is to determine the supplied flow rate to hydraulic swing motors such that the excavator follows the swing velocity command given by the human driver with a smooth acceleration/deceleration in spite of various uncertainties. Some of the difficulties in the design of such a high performance swing velocity tracking controller are: (i) The swing inertia is time-varying and unknown due to the movement of the linkage and the unknown payload in the bucket; (ii) Hydraulic parameters such as bulk modulus exhibits large variations during actual operation; (iii) The system is subjected to certain types of uncertain nonlinearities (e.g., leakage flows of swing motors) during normal operations on a flat ground; and (iv) The system may experience severe degree of uncertain nonlinearities when operating on a slope ground; the swing torque due to gravity forces on a slope surface is usually very large and changes quite rapidly. In this paper, by treating the supplied flow rate as the control input, a high performance nonlinear adaptive robust control algorithm is presented to address the control issues associated with the above several types of uncertainties all together at once. The presented scheme achieves a guaranteed transient as well as a guaranteed final tracking accuracy to satisfy the performance requirements of the application. In addition, asymptotic tracking is achieved in the presence of constant parametric uncertainties for an improved performance. Simulation results are presented to illustrate the proposed method.

*Part of the paper has been presented in 1998 American Control Conference. This work is funded by Caterpillar Inc. and in part by the National Science Foundation under the CAREER grant CMS-9734345

Nomenclature

$\dot{}$	dot overstrike represents the derivative of a variable
$\tilde{}$	tilde overstrike represents the estimation error of a parameter or a term
$\hat{}$	hat overstrike represents the estimate of a parameter or a term
$\{\bullet\}_d$	subscript d represents the desired value of a parameter/term $\bullet$
$\{\bullet\}_i$	subscript i represents the i-th element of $\bullet$
$\{\bullet\}_{max}$	subscript max represents an upper bound of $\bullet$
$\{\bullet\}_{min}$	subscript min represents a lower bound of $\bullet$
α	slope angle of ground
$\beta \in R^6$	lumped unknown physical quantities
β_e	bulk modulus of hydraulic fluid
b_c	coefficient of viscous friction force
C_{im}	internal leakage flow coefficient
$C_{emj}, j = 1, 2$	external leakage flow coefficients
$C_{sj}, j = 1, \ldots, 5$	some constants in choosing specific robust control terms
D_{mp}, D_m	constant coefficients of swing motors
e_ω	velocity tracking error
e_p	load pressure tracking error
$\varepsilon_\omega,\ \varepsilon_p$	small positive design parameters
F_c	Columb friction force
$\Gamma = diag\{\gamma_1, \ldots, \gamma_6\}$	diagonal adaptation rate matrix
I	swing inertia
ω	swing velocity
k_ω	positive velocity feedback gain
k_p	positive pressure feedback gain
m_L	inertia load in the bucket
ω_{input}	swing velocity commanded by the driver
P_L	load pressure of the swing motor
p_1	inlet pressure of the swing motor
p_2	outlet pressure of the swing motor
p_{ref}	tank reference pressure
P_s	pump supplied pressure
ΔP	pressure drop across the orifice of a controlled valve
Q_L	load flow rate of swing motor
Q_1	the supplied flow rate at the inlet of swing motor
Q_2	the flow rate at the outlet
Q_{loss}	flow loss
Q_{lossi}	internal or cross-port leakage flow
Q_{lossej}	external leakage flows
$q = [q_1, q_2, q_3]^T$	the vector of joint angles of the excavator arm
x_v	valve opening
T_e	torque due to reaction force of environment
T_{loss}	torque losses due to friction of the swing motor and gears
T_g	torque due to gravity forces on a slope ground
θ	swing angle
V_0	control volume of the swing motor
w_p	a positive weighting factor

1 INTRODUCTION

Hydraulic systems have been used in industry in a wide number of applications by virtue of their small size-to-power ratios and the ability to apply very large forces and torques. However, hydraulic systems also have a number of characteristics which complicate the development of high performance closed-loop controllers; dynamics of hydraulic systems are highly nonlinear [1] and have large extent of model uncertainties. Advanced control techniques have not been well developed to address these issues. This leads to the urgent need for advancing hydraulics technologies by combining the high power of hydraulic actuation with the versatility of advanced electronic control.

In the past, much of the work in the control of hydraulic systems uses linear control theory [2, 3, 4, 5, 6] and feedback linearization techniques [7, 8]. In [9], Alleyne and Hedrick applied the nonlinear adaptive control to the force control of an active suspension driven by a double-rod cylinder. They demonstrated that nonlinear control schemes can achieve a better performance than conventional linear controllers. They considered the parametric uncertainties of the cylinder only.

In [10], the adaptive robust control (ARC) approach proposed by Yao and Tomizuka in [11, 12, 13] was generalized to provide a rigorous theoretic framework for the high performance robust control of a one DOF electro-hydraulic servo-system by taking into account the particular nonlinearities and model uncertainties of the electro-hydraulic servo-systems. The effects of *parametric uncertainties* coming from both the inertia load and the cylinder and the *uncertain nonlinearities* such as friction forces were considered. The non-smoothness of nonlinearities associated with hydraulic dynamics (e.g., the nonlinear function describing the relationship between the flow rate and the valve opening) was carefully examined. A physical intuition based modification was provided to overcome the difficulty in carrying out the backstepping ARC design [12] caused by the non-smooth nonlinearities of the hydraulic dynamics.

In viewing the above recent developments in the nonlinear adaptive robust control of electro-hydraulic systems, it is natural to see if we can generalize the idea to the high performance control of future industrial hydraulic machines. As a stepping stone toward that goal, this paper focuses on some of the fundamental issues related to the design of high performance swing velocity tracking control algorithms for an industrial hydraulic excavator, one of the most commonly used earth-moving machines [14, 15, 16]. An industrial hydraulic excavator normally consists of a base supported by tracks, a rotating structure with a cab to hold the human driver, and a robot-arm-like three-DOF linkage (or boom, stick, and bucket called in hydraulic industry). The linkage is mounted on the rotating structure and is driven by three independent hydraulic cylinders to provide the necessary motion for digging and carrying and dumping the load in the bucket. The rotating structure is driven by hydraulic motors to provide swing motions. As a consequence, one of the fundamental issues in the swing motion control is to determine the supplied flow rate to the swing motors such that the resulting swing motion follows the swing velocity command given by the human driver with a smooth acceleration/deceleration in spite of various uncertainties. However, several difficulties exist in the development of such a high performance swing motion controller. First, the swing inertia is *time-varying* due to the movement of the linkage during swing motion and is *unknown* due to the unknown payload in the bucket. This makes the swing motion control theoretical

challenging; in principle, the approach in [10] can handle constant unknown inertia only and cannot be directly applied to the swing motion control. Second, the system has other *parametric uncertainties* (e.g., hydraulic parameters such as bulk modulus) and certain types of uncertain nonlinearities (e.g., leakage flows of swing motors) during normal operations on a flat ground. Third, the system may experience severe degree of uncertain nonlinearities when operating on an uneven ground; the swing torque due to gravity forces on a slope surface is usually very large and changes quite rapidly. Finally, the nominal swing motor operating pressure should not exceed the swing motor line relief pressure to avoid waste of energy.

In this paper, by treating the supplied flow rate as the control input, a high performance nonlinear adaptive robust control algorithm is presented to address the control issues caused by the types of uncertainties mentioned above. Thus the paper serves for two main purposes: one is to advance the design of high performance adaptive robust controllers (ARC) by addressing unsolved theoretical problems, and the other is to construct practical nonlinear adaptive robust controllers which are particularly suitable for the swing motion control of hydraulic excavators. Specifically, for the first purpose, a new ARC backstepping design will be developed to construct ARC controllers for a class of nonlinear systems whose state equations cannot be linearly parametrized by a suitably selected set of unknown constant parameters. In all the previously published work on ARC backstepping designs [12, 13, 10], the transformed state space equations are assumed to be linearly parametrized in terms of a suitably selected set of physical parameters; the assumption of linearly parametrizing state equation is also necessary for adopting any backstepping adaptive control designs presented in [17]. Thus, all existing backstepping ARC designs are restricted to the applications where only constant unknown inertia is involved as studied in [10]. In the current work, the swing inertia is time-varying and unknown. As a result, the resulting state equation *cannot* be linearly parametrized in terms of a suitably selected set of unknown constant parameters as shown later in the paper. Therefore, new adaptive robust control (ARC) design techniques have to be developed to overcome this practical and yet challenging theoretical problem. For the second purpose, several desirable ARC structures such as the ideas of the desired compensation ARC [18] and the discontinuous projection based ARC [13] will be integrated in the development of the proposed high performance swing motion tracking controller.

2 DYNAMIC MODEL OF SWING CIRCUIT

For this initial investigation, we consider the two major components of the swing circuit only: (i) Rotating Structure of the Excavator; and (ii) Swing Motors. Other related components such as valves and the pump are neglected; their effects will be considered in the future work. The analytical model of each individual element is given below.

2.1 Dynamic Model of Excavator Swing Motion

The excavator swing motion can be described by

$$I(t)\dot{\omega} = D_{mp}P_L - \dot{I}\omega - T_{loss} - T_e + T_g \tag{1}$$

where $\omega = \dot{\theta}$ represents the swing velocity, θ is the swing angle, I is the swing inertia, $P_L = p_1 - p_2$ is the load pressure built up in the swing motors, D_{mp} is a constant coefficient, $\dot{I}\omega$ is the torque due to the change of swing inertia, $T_{loss} = b_c\omega + F_c sign(\omega)$ is the torque losses due to friction of the swing motor and gears, in which b_c represents the coefficient of the viscous friction forces including swing motor torque losses and F_c is the Columb friction force, T_e represents the torque due to the reaction forces of the contacting environment (e.g., the torque due to the reaction force of a wall when the excavator arm hits a wall), and T_g is the torque due to gravity forces on a slope ground.

The detailed expressions of $I(t)$ and T_g are given in [19], from which the following general statements can be said. The swing inertia I consists of three parts given by

$$I = I_1 + I_2(q(t)) + I_3(q(t), m_L) \tag{2}$$

where I_1 is the swing inertia due to the rotating structure with the cab, which is *constant*, I_2 is the swing inertia due to the boom, stick, and bucket, which is a function of the link position $q = [q_1, q_2, q_3]^T \in R^3$ and thus *time-varying* when the link is actuated during the swing motion, and I_3 is the swing inertia due to the inertia load in the bucket, which is a function of the link position q and the mass of the inertia load m_L ; m_L is normally unknown.

The gravitational torque T_g is a function of the ground slope angle α, the swing angle θ, the link position q, and the mass of the inertia load m_L, i.e., $T_g = T_g(\alpha, \theta, q, m_L)$. Since the swing angle θ and the ground slope angle α are not measured, T_g is unknown, which increases the controller design difficulty. T_g is zero on a level ground, i.e., $T_g = 0$ when $\alpha = 0$.

2.2 Dynamic Model of Swing Motors

Assume that the volume ripple of the motor is small compared to the total control volume V_0. V_0 includes the volumes due to valves, connecting lines/manifold, motor passage, and the volume swept out by the swing motor pistons or vanes. The swing motor can be described by [1]

$$\begin{aligned} \tfrac{V_0}{\beta_e}\dot{p}_1 &= Q_1 - D_m\omega - Q_{lossi}(\omega, p_1, p_2) - Q_{losse1}(\omega, p_1) \\ \tfrac{V_0}{\beta_e}\dot{p}_2 &= -Q_2 + D_m\omega + Q_{lossi}(\omega, p_1, p_2) - Q_{losse2}(\omega, p_2) \end{aligned} \tag{3}$$

where p_1 and p_2 are the inlet and outlet pressures of the swing motor respectively, β_e is the bulk modulus of hydraulic fluid, Q_1 is the supplied flow rate at the inlet; positive for the flow in and negative for the flow out, Q_2 is the supplied flow rate at the outlet; positive for the flow out and negative for the flow in,

D_m is a constant efficient, Q_{lossi} represents the internal or cross-port leakage flow; a simplified model is given by $Q_{lossi} = C_{im}(p_1 - p_2)$, and $Q_{lossej}, j = 1, 2$, represent the external leakage flows; a simplified model is given by $Q_{lossej} = C_{emj}(p_j - p_{ref})$ where p_{ref} is the tank reference pressure.

Define the load flow rate Q_L to be $Q_L = Q_1$ if the inlet of the swing motor is the port to be controlled[1], and to be $Q_L = Q_2$ if the outlet of the swing motor is the port to be controlled. Consequently, $P_L = p_1 - p_{ref}$ if $Q_L = Q_1$, and $P_L = p_{ref} - p_2$ if $Q_L = Q_2$. From (3), the load pressure P_L is related to the load flow rate Q_L by

$$\frac{V_0}{\beta_e}\dot{P}_L = Q_L - D_m\omega - Q_{loss}(\omega, p_1, p_2) \tag{4}$$

where Q_{loss} is the flow loss defined to be $Q_{loss} = Q_{lossi} + Q_{losse1}$ for $Q_L = Q_1$ and $Q_{loss} = Q_{lossi} - Q_{losse2}$ for $Q_L = Q_2$.

In practice, the load flow rate Q_L is controlled by a set of valves, and is related to the valve opening x_v and the pressure drop ΔP across the orifice of the controlled valve by certain static nonlinear mappings [1], i.e., $Q_L(x_v, \Delta P)$. For the system that is studied in this paper, the pressure drop ΔP is measured and is known. Thus, the correct valve opening that is needed to supply a requested desired load flow rate Q_{Ld} can be backed out by using the inverse of the nonlinear flow mapping as $x_v = Q_L^{-1}(Q_{Ld}, \Delta P)$. Furthermore, if the nonlinear flow mapping has large degree of uncertainties and the bandwidth of valve dynamics are not so high to be neglected, the backstepping ARC design with the consideration of valve dynamics proposed in [10] and the backstepping ARC design developed later in this paper may be integrated to solve the problem of robust control of valves for a requested load flow rate. Therefore, for simplicity, in this paper, the load flow rate Q_L will be treated as the control input so that we can focus on the control issues associated with the swing motion (1) and the swing motor dynamics (4) and the dynamic interaction between them. *The control objective can thus be stated as that of designing a control law for Q_L such that the resulting swing velocity ω tracks any feasible desired swing velocity trajectory $\omega_d(t)$ as closely as possible in spite of various uncertainties in the swing motion equation (1) and the swing motor equation (4).*

3 SWING VELOCITY TRACKING CONTROL STRATEGY

In free space, $T_e = 0$, and a swing velocity control strategy is needed to determine the supplied flow rates to the swing motors such that the resulting excavator swing motion follows the driver's velocity command. The proposed strategy consists of two parts: (i) On-line desired velocity trajectory generation, and (ii) Velocity tracking controller. Overall controller structure and the resulting closed-loop system is shown in Fig.1

III.1 On-line Desired Velocity Trajectory Generation

[1]In such a case, the outlet port of the motor is not controlled and is left wide open such that $p_2 = p_{ref}$

This block is to provide a feasible desired velocity trajectory $\omega_d(t)$ that the swing circuit can track. The purpose is to achieve a smooth acceleration/deceleration and pressure limiting. A by-product of this on-line algorithm is that we can use trajectory initialization to reduce transient response of the velocity tracking controller as seen later.

If not controlled properly, swing motor pressures normally reach to line-relief pressures during transient periods when the acceleration/deceleration are large, which are physically intuitive as explained as follows. In (1), during transient periods when $|\dot{\omega}|$ is large, terms like $\dot{I}\omega$, T_{loss}, and T_g are relatively small, and the load pressure P_L mainly depends on the inertia load $I\dot{\omega}$. So for pressure limiting, it is necessary to limit the acceleration/deceleration that the system is supposed to track, which can be achieved by choosing a suitable value for the maximal allowable desired acceleration $\dot{\omega}_M$. For example, a conservative $\dot{\omega}_M$ can be chosen such that

$$\dot{\omega}_M = \frac{1}{I_{max}} \left[D_{mp} P_{Lmax} - \{\dot{I}\omega + T_{loss} - T_g\}_{max} \right] \tag{5}$$

where I_{max} is the largest possible swing inertia that the system is expected to encounter, P_{Lmax} is the maximal allowable working pressure, and $\{\bullet\}_{max}$ represents the conservative upper bound of $\bullet$ during all possible working ranges.

For driver's comfort, sometimes, it may be desirable to limit the rate of pressure change. By differentiating (1) and using similar intuitive arguments as in the above for pressure limiting, it can be seen that $\dot{P}_L$ mainly depends on $I\ddot{\omega}$ during transient periods. Thus, the rate of pressure change can be indirectly regulated by limiting the jerk of the desired trajectory below a maximal allowable jerk $\ddot{\omega}_M$. For example, a conservative bound can be chosen as

$$\ddot{\omega}_M = \frac{1}{I_{max}} \left[D_{mp} \dot{P}_{Lmax} - \{\ddot{I}\omega + 2\dot{I}\dot{\omega} + \dot{T}_{loss} - \dot{T}_g\}_{max} \right] \tag{6}$$

where $\dot{P}_{Lmax}$ is the maximal allowable pressure changing rate.

Let $\omega_{input}(t)$ be the swing velocity commanded by the driver. The desired swing velocity trajectory $\omega_d(t)$ is generated through a second-order filter [2] with an acceleration and jerk limit, i.e.,

$$\ddot{\omega}_d(t) = -2\zeta_t \omega_t \dot{\omega}_d(t) - \omega_t^2 (\omega_d(t) - \omega_{input}(t)) \tag{7}$$

with the constraints that $|\dot{\omega}_d| \leq \dot{\omega}_M$ and $|\ddot{\omega}_d| \leq \ddot{\omega}_M$; the detailed trajectory generation algorithm which achieves this goal can be found in [19]. The initial values $\omega_d(0)$ and $\dot{\omega}_d(0)$ will be chosen later to minimize the transient response.

III.2 Velocity Tracking Controller

III.2.1 Controller Design Models

[2] ω_t and ζ_t represent the natural frequency and the damping ration of the second-order filer

The closed-loop velocity tracking control law will be synthesized based on the physical models presented in section II. From (2), the swing inertia can be separated into two parts given by

$$I = I_c(q(t)) + I_{c\beta}(q(t))m_L \tag{8}$$

where $I_c(q(t))$ and $I_{c\beta}(q(t))$ can be calculated based on the link configuration $q(t)$; the analytical expressions for the calculation are given in [19] and in section IV. The physical model (1) and (4) can be rewritten in the following form for controller design:

$$\begin{aligned} &I(t)\dot{\omega} = D_{mp}P_L - (\dot{I}_c + \dot{I}_{c\beta}\beta_1)\omega - \hat{T}_{loss} + \beta_2, \qquad I = I_c + I_{c\beta}\beta_1 \\ &\dot{P}_L = \beta_3[Q_L - D_m\omega - \hat{Q}_{loss}] + \beta_4 \end{aligned} \tag{9}$$

where $\hat{T}_{loss}$ and $\hat{Q}_{loss}$ are any estimates of torque losses and flow losses respectively, which can be chosen to be zero to reduce the complexity of the resulting controller as done in the simulation. The lumped unknown physical quantities β_1, β_2, β_3, and β_4 are defined as

$$\begin{aligned} &\beta_1 = m_L \\ &\beta_2 = \tilde{T}_{loss} + T_g, \qquad \tilde{T}_{loss} = \hat{T}_{loss} - T_{loss} \\ &\beta_3 = \tfrac{\beta_e}{V_0} \\ &\beta_4 = \tfrac{\beta_e}{V_0}\tilde{Q}_{loss} \qquad \tilde{Q}_{loss} = \hat{Q}_{loss} - Q_{loss} \end{aligned} \tag{10}$$

For controller design purpose, we also define β_5 and β_6 as

$$\begin{aligned} &\beta_5 = \beta_1\beta_3 = m_L\tfrac{\beta_e}{V_0} \\ &\beta_6 = \beta_1\beta_4 = m_L\tfrac{\beta_e}{V_0}\tilde{Q}_{loss} \end{aligned} \tag{11}$$

which represent the coupling effect between the unknown inertia load and the unknown swing motor parameters.

Assumptions:

The following reasonable assumptions are made:

- **A1** Valves and pumps can provide the synthesized control flow rate Q_L;
- **A2** Swing velocity and swing motor pressures are measured, i.e., ω, p_1, and p_2 are measured;
- **A3** Physical quantities $\beta(t)$ are bounded with known bounds, i.e., $\beta_{min} \le \beta(t) \le \beta_{max}$, where $\beta_{min} = [\beta_{1min}, \ldots, \beta_{6min}]^T$ and $\beta_{max} = [\beta_{1max}, \ldots, \beta_{6max}]^T$ are known;
- **A4** Positions, velocities, and acceleration of boom, stick, and bucket (i.e., $q(t)$, $\dot{q}(t)$, and $\ddot{q}(t)$) are available for the calculation of known parts of the swing inertia and their derivatives, i.e., I_c and $I_{c\beta}$ in (8) and their derivatives $\dot{I}_c$, $\dot{I}_{c\beta}$, $\ddot{I}_c$, and $\ddot{I}_{c\beta}$ can be calculated.

Justification of Assumptions:

i As explained in section II.B, for simplicity, the load flow rate Q_L is treated as the control input in this paper. Thus, Assumption A1 is necessary for one to start a control design.

ii Assumption A2 is satisfied by the current hardware setting of an excavator that we are working on.

iii Assumption A3 is practically reasonable since physically all terms involved in β are bounded and we know the extent of model uncertainties the system is going to handle; for example, the lower bound of the inertia load β_1 will be zero and the upper bound will be the maximal load that the bucket can hold.

iv Assumption A4 is reasonable since the arm configuration $q(t)$ can be obtained by either using joint angle sensors mounted at each joint of the excavator arm or using the cylinder displacement sensors mounted at the boom, stick, and bucket hydraulic cylinders respectively. Joint velocity $\dot{q}(t)$ and acceleration $\ddot{q}(t)$ can then be obtained by differentiating $q(t)$ with filters. Since $\dot{q}(t)$ and $\ddot{q}(t)$ are only used to calculate the known parts of the swing inertia and their derivatives for a better model compensation, the small amount of phase delay introduced by the filters in obtaining $\dot{q}(t)$ and $\ddot{q}(t)$ may not affect the stability of the resulting system much, and thus will not be a serious issue. In addition, Assumption A4 can be removed at the expense of a degraded performance where no swing inertia compensation will be used.

III.2.2 Control Design Difficulties

At this stage, it is ready to see that some of the difficulties in designing a stable and high performance controller for (9) and (10) are:

D1 . The system may experience large variations of inertia load and hydraulic parameters such as bulk modulus, which are represented by β_1 and β_3 in (10).

D2 . The system is subjected to certain degree of uncertain nonlinearities such as the leakage flows and the friction torque losses during normal operations when $T_g = 0$; these effects are represented by β_2 and β_4 in (10).

D3 . On a slope ground, the system may experience large rapid changing swing torque $T_g(\alpha, \theta, q, m_L)$, which is represented by $\beta_2(t)$ in (10).

D4 . From (9), the state equation for $\dot{\omega}$ is

$$\dot{\omega} = \frac{1}{I_c(t)+I_{c\beta}(t)\beta_1}\left[D_{mp}P_L - (\dot{I}_c(t) + \dot{I}_{c\beta}(t)\beta_1)\omega - \hat{T}_{loss} + \beta_2\right] \tag{12}$$

which cannot be linearly parametrized in term of a suitably selected set of unknown physical quantities since $I_c(t)$ and $I_{c\beta}(t)$ in (12) are time-varying when the link is actuated during swing motion. This prohibits the direct applications of the existing nonlinear adaptive robust control (ARC) schemes [13, 10] since all those schemes need the state equation to be linearly parametrized by a set of unknown constant quantities; linearly parametrizing state equations is also necessary

for adopting any backstepping adaptive control designs presented in [17]. Thus, novel backstepping ARC designs have to be developed to address this unsolved theoretical problem. In the following, this problem is solved by using a Lyapunov function V containing the unknown swing inertia $I(t)$ as a weighting factor and certain re-parametrization techniques to linearly parametrize the derivative of the Lyapunov function V instead of the state-equation (12). The proposed re-parametrization technique needs the introduction of the coupling quantities β_5 and β_6 given by (11).

III.2.3 Novel Adaptive Robust Control Designs

In this subsubsection, a novel backstepping ARC design procedure is developed to obtain a velocity tracking control algorithm to address the control difficulties stated in III.2.2. The design consists of two steps as follows, which reflects the fact that the control flow rate Q_L affects the actual swing velocity through two first-order differential equations shown in (9) and in Fig.1.

Step 1:

The swing motion is produced by the motor pressure P_L as described by the first equation of (9), which is also graphically shown in Fig.1. So the first step is to design a desired load pressure P_{Ld} for P_L so that any feasible desired velocity trajectory $\omega_d(t)$ can be tracked when $P_L = P_{Ld}$. This can be accomplished by applying the adaptive robust control strategy in [13] and dissipating an energy-like positive function given by

$$V_1 = \tfrac{1}{2} I(t) e_\omega^2 \tag{13}$$

where $e_\omega = \omega - \omega_d$ is the velocity tracking error. For simplicity, in the following, $\hat{\bullet}$ is used to represent the estimate of $\bullet$ by substituting the parameter estimate $\hat{\beta}$ for β in the expression of $\bullet$, $\tilde{\bullet} = \hat{\bullet} - \bullet$ for the estimation error, $\bullet_{max}$ (or $\bullet_{min}$) for the maximum (or minimum) value of $\bullet$, and $\bullet_j$ for the j-th element of the vector $\bullet$. The absolute operation $|\bullet|$ for a vector is performed elementally.

Lemma 1 *Let the desired control function for the load pressure P_L be*

$$\begin{aligned} P_{Ld} &= P_{Lda}(\omega, \hat{\beta}, \omega_d, \dot{\omega}_d, q(t)) + P_{Lds}(\omega, \hat{\beta}, \omega_d, \dot{\omega}_d, q(t)) \\ P_{Lda} &= \tfrac{1}{D_{mp}} \left[\hat{\dot{I}} \omega_d + \hat{I} \dot{\omega}_d + \hat{T}_{loss} - \hat{\beta}_2 - k_\omega I_c(t) e_\omega \right] \end{aligned} \tag{14}$$

where $k_\omega > 0$ is a feedback gain, and P_{Lds} is any robust control term satisfying the following two conditions:

$$\begin{aligned} &i. \quad e_\omega \left[D_{mp} P_{Lds} - \phi_{\omega 1} \tilde{\beta}_1 - \tilde{\beta}_2 \right] \le \varepsilon_\omega \\ &ii. \quad e_\omega D_{mp} P_{Lds} \le 0 \end{aligned} \tag{15}$$

in which $\varepsilon_\omega > 0$ is a design parameter, and $\phi_{\omega 1}$ is defined by

$$\phi_{\omega 1}(t) \triangleq -(\dot{I}_{c\beta} \omega_d + I_{c\beta} \dot{\omega}_d) \tag{16}$$

If the feedback gain k_ω is large enough such that $2k_\omega I_c + \dot{I} > 0$, then,

a) . In general,

$$\dot{V}_1 \mid_{e_p=0} \quad \leq -\lambda_{V1} V_1 + \varepsilon_\omega \tag{17}$$

where the short-hand notation $\dot{V}_1 \mid_{e_p=0}$ represents the derivative of V_1 when the load pressure tracking error $e_p = P_L - P_{Ld}$ is zero, and λ_{V1} is the largest positive scalar satisfying $\lambda_{V1} \leq \frac{2k_\omega I_c + \dot{I}}{I}$.

b) . In addition,

$$\dot{V}_1 \mid_{e_p=0} \quad \leq -\lambda_{V1} V_1 + e_\omega \left[-\phi_{\omega 1} \tilde{\beta}_1 - \tilde{\beta}_2 \right] \tag{18}$$

□

Proof of Lemma 1 is given in Appendix P1.

Remark 1 *Result a) of Lemma 1 implies that, if $e_p = 0$, i.e., the desired load pressure P_{Ld} can be delivered, then,*

$$V_1 \quad \leq exp(-\lambda_{V1} t) V_1(0) + \tfrac{\varepsilon_\omega}{\lambda_{V1}} [1 - exp(-\lambda_{V1} t)] \tag{19}$$

which means that V_1 exponentially converges to a small ball: $\{V_1 : \ V_1 \leq \frac{\varepsilon_\omega}{\lambda_{V1}}\}$, whose size can be freely adjusted by decreasing the design parameter ε_ω and/or increasing k_ω (which increases λ_{V1}) in a known form. In other words, transient performance and final tracking accuracy is guaranteed in general since V_1 is a positive definite function of the velocity tracking error e_ω. As seen later, Result b) of Lemma 1 implies that adding proper parameter adaptation will enable us to reduce parametric uncertainties to further improve tracking accuracy [13]. ♢

Remark 2 *In Lemma 1, the robust control term P_{Lds} is required to satisfy the two constraints in (15); the first constraint reflects the fact that the robust control term P_{Lds} should be chosen in a way that the effect of all related model uncertainties is attenuated to a controllable degree measured by the design parameter ε_ω, and the second constraint is to make sure that the robust control term is passive. In general, robust control terms satisfying constraints like (15) are not unique. General ways to choose the needed robust control term can be referred to [12, 13]. One specific P_{Lds} which is suitable for this particular application is given by*

$$P_{Lds} = -\tfrac{1}{D_{mp}} C_{s1} e_\omega^3 \tag{20}$$

where $C_{s1} > 0$ is a positive scalar. It is proven in Appendix P2 that P_{Lds} given by (20) satisfies the constraints (15) with the property that a larger C_{s1} results in a smaller ε_ω. ♢

Remark 3 *In (14), P_{Ld} consists of model compensation (the first four terms of P_{Lda}), a simple proportional feedback control law with a time-varying gain $k_\omega I_c(t)$, and a nonlinear robust feedback term P_{Lds}, which is graphically illustrated in Fig.2. The purpose of using a time-varying linear gain $k_\omega I_c(t)$ is to achieve a constant bandwidth over a large operating range since the swing inertia I changes with the link configuration. It is also seen that the model compensation part is of the desired compensation*

structure [18] (i.e., the model compensation can be calculated based on the desired trajectory $\omega_d(t)$ and the parameter estimates only). Desired model compensation structure reduces the effect of measurement noise [20, 21] and improves tracking accuracy in general, which has been experimentally verified for other applications such as the motion control of robot manipulators [18]. $\diamondsuit$

Step 2:

As seen from Lemma 1, if the load pressure tracks the desired load pressure P_{Ld} given by (14), then, the resulting swing velocity will track its desired trajectory and we would achieve our goal. Thus, the second step is to design a desired flow rate Q_{Ld} for Q_L so that the actual load pressure P_L tracks the desired load pressure P_{Ld}; this step is based on the swing motor equation (the second equation of (9)) and the design is accomplished by dissipating a total-energy-like positive function given by

$$V = V_1 + \tfrac{1}{2} w_p I e_p^2 \tag{21}$$

where w_p is a positive weighting factor. For simplicity, we subsequently define the following terms,

$$\begin{aligned}
\widehat{I\dot{P}_{Ld}} &\triangleq \tfrac{\partial P_{Ld}}{\partial \omega}(D_{mp}P_L - \hat{\dot{I}}\omega - \hat{T}_{loss} + \hat{\beta}_2) + \hat{I}\tfrac{\partial P_{Ld}}{\partial t} \\
\alpha_{2c} &\triangleq -\tfrac{1}{w_p} D_{mp} e_\omega - I_c\hat{\beta}_4 - I_{c\beta}\hat{\beta}_6 + \widehat{I\dot{P}_{Ld}} \\
\alpha_{2cq} &\triangleq \tfrac{1}{I_c\hat{\beta}_3 + I_{c\beta}\hat{\beta}_5}(\alpha_{2c} - k_p I_c(t) e_p) \\
\phi_p &\triangleq \begin{bmatrix} \frac{\partial P_{Ld}}{\partial \omega}\dot{I}_{c\beta}\omega - I_{c\beta}\frac{\partial P_{Ld}}{\partial t} \\ -\frac{\partial P_{Ld}}{\partial \omega} \\ I_c\alpha_{2cq} \\ I_c \\ I_{c\beta}\alpha_{2cq} \\ I_{c\beta} \end{bmatrix} \\
\tau_\beta &\triangleq \begin{bmatrix} e_\omega\phi_{\omega 1} \\ e_\omega \\ 0 \\ 0 \\ 0 \\ 0 \end{bmatrix} + w_p e_p \phi_p
\end{aligned} \tag{22}$$

in which k_p in the expression of α_{2cq} is a positive feedback gain.

Theorem 1 *Let the adaptation law be*

$$\dot{\hat{\beta}} = Proj\left(\Gamma\tau_\beta(\omega, P_L, \hat{\beta}, \omega_d, \dot{\omega}_d, \ddot{\omega}_d, q, \dot{q}, \ddot{q}\right) \tag{23}$$

where $\Gamma = diag\{\gamma_1, \ldots, \gamma_6\} > 0$ is any diagonal adaptation rate matrix, Proj represents the widely used projection mapping [22, 11, 13], and the adaptation function τ_β is defined in (22). Choose the control law as

$$\begin{aligned}
Q_L &= Q_{Lda}(\omega, P_L, \hat{\beta}, \omega_d, \dot{\omega}_d, \ddot{\omega}_d, q, \dot{q}, \ddot{q}) + Q_{Lds}(\omega, P_L, \hat{\beta}, \omega_d, \dot{\omega}_d, \ddot{\omega}_d, q, \dot{q}, \ddot{q}) \\
Q_{Lda} &= D_m\omega + \hat{Q}_{loss} + \alpha_{2cq}
\end{aligned} \tag{24}$$

where α_{2cq} is defined in (22), and Q_{Lds} is any robust control term satisfying the following two conditions

$$\begin{aligned} &i. \quad w_p e_p \left\{ I\beta_3 Q_{Lds} - \phi_p^T \tilde{\beta} - I\frac{\partial P_{Ld}}{\partial \hat{\beta}_1}\dot{\hat{\beta}}_1 - I\frac{\partial P_{Ld}}{\partial \hat{\beta}_2}\dot{\hat{\beta}}_2 \right\} \le \varepsilon_p + I_c(\tfrac{1}{2}k_\omega e_\omega^2 + \tfrac{1}{2}k_p w_p e_p^2) \\ &ii. \quad w_p e_p \left\{ I\beta_3 Q_{Lds} - I\frac{\partial P_{Ld}}{\partial \hat{\beta}_1}\dot{\hat{\beta}}_1 - I\frac{\partial P_{Ld}}{\partial \hat{\beta}_2}\dot{\hat{\beta}}_2 \right\} \le I_c(\tfrac{1}{2}k_\omega e_\omega^2 + \tfrac{1}{2}k_p w_p e_p^2) \end{aligned} \tag{25}$$

where ε_p is a positive design parameter. If feedback gains k_ω and k_p are large enough such that $k_\omega I_c + \dot{I} > 0$ and $k_p I_c - \dot{I} > 0$, then,

a) . In general, the closed-loop system is globally stable with V bounded above by

$$V \quad \le exp(-\lambda_V t)V(0) + \tfrac{\varepsilon_V}{\lambda_V}[1 - exp(-\lambda_V t)] \tag{26}$$

where λ_V is the largest positive scalar satisfying $\lambda_V \le min\{\frac{k_\omega I_c + \dot{I}}{I},\ \frac{k_p I_c - \dot{I}}{I}\}$, and $\varepsilon_V = \varepsilon_\omega + \varepsilon_p$.

b) . In addition, in the presence of constant parametric uncertainties only, i.e., β being unknown but constant, asymptotic output tracking (or zero final tracking error) is achieved.

c) . Furthermore, if the initial values, $\omega_d(0)$ and $\dot{\omega}_d(0)$, for the desired trajectory generation algorithm in section III.1 are chosen as

$$\begin{aligned} \omega_d(0) &= \omega(0) \\ \dot{\omega}_d(0) &= \tfrac{1}{I}\left[D_{mp}P_L - \dot{\hat{I}}\omega - \hat{T}_{loss} + \hat{\beta}_2 \right] |_{t=0} \end{aligned} \tag{27}$$

where all terms in the right hand sides of (27) are evaluated at $t = 0$, then, $V(0) = 0$, and thus transient response is minimized as seen from (26). □

Proof of Theorem 1 is given in Appendix P3.

Remark 4 *From (21), $V \ge \frac{1}{2}Ie_\omega^2$. Result a) of Theorem 1 thus implies that $|e_\omega(\infty)| \le \frac{1}{I}\sqrt{\frac{2\varepsilon_V}{\lambda_V}}$. Furthermore, the bound of the final output tracking error, $\frac{1}{I}\sqrt{\frac{2\varepsilon_V}{\lambda_V}}$, can be made arbitrarily small by decreasing ε_ω and ε_p, which will result in a smaller ε_V, and/or increasing feedback gains k_ω and k_p, which will result in a larger λ_V. (26) also indicates that the proposed controller has an exponentially converging transient performance with the exponentially converging rate λ_V being able to be adjusted via certain controller parameters freely; such a guaranteed transient performance is especially important for practical applications (e.g., swing control) since execute time is normally short. Theoretically, this result is what a well-designed robust controller can achieve.*

Theoretically, Result b) of Theorem 1 is what a well-designed adaptive controller can achieve. Practically, this result implies that even a low bandwidth controller (feedback gains are not so large) may have a very small tracking error due to the reduced parametric uncertainties. This is a nice feature for the swing velocity control since actual valve's bandwidth may be low and sampling rate may not be so fast, which limit the bandwidth that the nominal closed-loop system can be placed without running into stability problem in the presence of those neglected dynamics in practice. ♢

Remark 5 *Similar to Remark 2, in Theorem 1, the choice of robust control term Q_{Lds} satisfying (25) is not unique. A specific form of Q_{Lds}, which may be suitable for this particular application, is given by*

$$\begin{aligned} Q_{Lds} = -\Big\{ & C_{s2}\left(\gamma_1 |\frac{\partial P_{Ld}}{\partial \hat{\beta}_1}||\phi_{\omega 1}| + \gamma_2 |\frac{\partial P_{Ld}}{\partial \hat{\beta}_2}|\right)^2 + C_{s3}\left(\gamma_1 |\frac{\partial P_{Ld}}{\partial \hat{\beta}_1}||\phi_{p1}|\right. \\ & \left. + \gamma_2 |\frac{\partial P_{Ld}}{\partial \hat{\beta}_2}||\phi_{p2}|\right) - C_{s4} I_c + C_{s5}\left(|\phi_p|^T \beta_M\right)^2 \Big\} e_p \end{aligned} \tag{28}$$

where ϕ_{p1} and ϕ_{p2} are the first and second element of the vector ϕ_p defined in (22) respectively, and C_{sj} are constants given by $C_{s2} = w_p I_{max}/(2k_\omega I_{min}\beta_{3min})$, $C_{s3} = w_p/\beta_{3min}$, $C_{s4} = k_p/(2I_{max}\beta_{3max})$, and $C_{s5} = w_p/(4I_{min}\beta_{3min}\varepsilon_p)$. It is shown in Appendix P4 that (25) is satisfied by (28). ♢

4 Simulation Results

A simulation program has been developed to simulate the performance of the proposed swing control strategy. The units shown in Table 1 are used to normalize different quantities to minimize the effect of numerical calculation error.

Physical parameters used in the swing motion (1) and the swing motor (3) are obtained from the specification of an industrial hydraulic excavator manufactured by Caterpillar Inc., which are tabulated in Table 2, in which the following short hand notations are used: $C_{q1} = cos(q_1)$, $S_{q1} = sin(q_1)$, $C_{q12} = cos(q_1+q_2)$, $S_{q12} = sin(q_1+q_2)$, $C_{q123} = cos(q_1+q_2+q_3)$, and $S_{q123} = sin(q_1+q_2+q_3)$.

Quantity	*Unit*
Pressure	bar
Flow Rate	L/min
Swing Velocity	rad/s
Torque	kN
Mass	$1000kg$
Length	m

Table 1: Units of Various Physical Quantities

As mentioned in section II.B, in implementation, the control flow rates are supplied by a set of valves. Thus, in the simulation, the effect of valve dynamics is also considered. Experimental tests showed that the valve dynamics (from the commanded input current to the valve to the actual valve opening x_v) can be described by a second-order transfer function with a break frequency of ω_v and a damping ratio of ζ_v. A relative high break frequency of $\omega_v = 50Hz$ and a damping ratio of $\zeta_v = 0.71$ are used in the simulation so that the effect of valve dynamics can be safely neglected in the controller design stage as done in the paper. If the actual valve's bandwidth is not high enough, linear control techniques may be used to raise the bandwidth of the valve first since the actual valve dynamics are normally quite linear and invariant. A sampling rate of $200Hz$ is used in the simulation.

Quantity	*Actual Value or Expression*
I	$I_c + I_{c\beta} m_L$
I_c	$123 + 15.7C_{q1} - S_{q1} + 206.2C_{q1}^2 - 15.1C_{q1}S_{q1} + 1.5S_{q1}^2 + 3.66C_{q12} - 0.17S_{q12}$ $+115C_{q1}C_{q12} - 5.4C_{q1}S_{q12} + 25C_{q12}^2 - 0.75C_{q12}S_{q12} + 0.2S_{q12}^2 + 0.69C_{q123}$ $-0.01S_{q123} + 21.6C_{q1}C_{q123} - 0.34C_{q1}S_{q123} + 10.8C_{q12}C_{q123}$ $-0.17C_{q12}S_{q123} + 1.23C_{q123}^2 - 0.04C_{q123}S_{q123} + 0.0003S_{q123}^2$
$I_{c\beta}$	$0.053 + 3.3C_{q1} + 1.65C_{q12} + 0.38C_{q123} - 0.006S_{q123} + 51.8C_{q1}^2 + 51.8C_{q1}C_{q12}$ $+11.85C_{q1}C_{q123} - 0.19C_{q1}S_{q123} + 12.96C_{q12}^2 + 5.93C_{q12}C_{q123}$ $-0.09C_{q12}S_{q123} + 0.68C_{q123}^2 - 0.02C_{q123}S_{q123} + 0.00017S_{q123}^2$
m_L	3
D_{mp}	0.8185
b_c	28.4
F_c	8.652
T_g	$\{[(35.2 + 34.3C_{q1} - 2.2S_{q1} + 8C_{q12} - 0.37S_{q12} + 1.5C_{q123} - 0.024S_{q123})$ $+m_L(0.23 + 7.2C_{q1} + 3.6C_{q12} + 0.82C_{q123} - 0.01S_{q123})]\, sin(\theta)$ $+(0.2 + 0.03m_L)cos(\theta)\}\, gsin(\alpha)$
V_0	95.008
β_e	2625
D_m	491.1
C_{im}	0.0584
$C_{em1} = C_{em2}$	0.05572
P_s	255
p_{ref}	1

Table 2: Physical Parameters of Swing Motion and Motors

Purpose	*Parameter Values*
Inertia estimate	$\hat{m}_L = 0$
Torque loss estimate	$\hat{b}_c = 0,\ \hat{F}_c = 0$
Flow loss estimate	$\hat{C}_{im} = 0\ ,\ \hat{C}_{em1} = \hat{C}_{em2} = 0$
Bulk modulus estimate	$\hat{\beta}_e = 4\beta_e$
Physical bounds	$\beta_{min} = [0, -100, 27.6, -4421, 0, -15030]^T$
	$\beta_{max} = [3.4, 100, 110.5, 4421, 375.8, 15030]^T$
	$I_{max} = 752, \quad I_{min} = 130$
Velocity trajectory planning	$\omega_t = 18.85,\ \zeta_t = 1,\ \dot{\omega}_M = 0.2177,\ \ \ddot{\omega}_M = 5.44$
Velocity tracking controller	$k_\omega = 62.8,\ \ k_p = 62.8,\ \ w_p = 4 \times 10^{-5}\ ,\ \ C_{s1} = 1.63 \times 10^7,\ \varepsilon_p = 100$
	$\Gamma = diag\{442, 2 \times 10^4,\ 1.1 \times 10^4, 2.7 \times 10^8, 4.26 \times 10^4, 10^9\}$

Table 3: Controller Parameter Values

Although simulation has been carried out for various operating conditions, due to space limit, only the following typical operation is shown here. During the first 5 seconds of the simulation, the driver's commanded velocity is assumed to be $\omega_{input} = 0.5 rad/s$, which is near the full speed of the excavator. After that, the driver's commanded velocity is zero. To see the effect of fast changing link configuration, the movement of boom, stick, and bucket is assumed to be described by $q = [30^o + 15^o(1 - cos(\frac{\pi}{4}t)),\ 120^o - 30^o(1 - cos(\frac{\pi}{4}t)),\ 90^o - 45^o(1 - cos(\frac{\pi}{4}t))]^T$.

The controller parameters used in the simulation are summarized in Table 3. As seen, the estimated torque loss and flow loss are assumed to be zero to simplify the resulting controller and to test the robustness of the algorithm. Large parameter estimation errors for physical parameters like m_L and β_e are also assumed as shown in Table 3 to test the effectiveness of using parameter adaptation.

The desired velocity trajectory profile and the actual velocity are shown in Fig.3. As shown, the desired velocity trajectory approaches to the driver's command smoothly and the actual velocity follows the desired velocity very closely to achieve a smooth acceleration and deceleration. This verifies the velocity tracking capability of the proposed ARC strategy in spite of various model uncertainties. Furthermore, the working pressures shown in Fig.4 verify that the working pressures did not exceed the line relief pressure. All these show that the proposed strategy achieves the objectives set forth under the assumed conditions.

To see the effect of parameter adaptation, we re-run the simulation but without using parameter adaptation. In such a case, the control law is equivalent to a deterministic robust control (DRC) law [11, 12]. The tracking errors e_ω are shown in Fig. 5 for both ARC and DRC. It can be seen that ARC achieves a better tracking performance than DRC due to the use of parameter adaptation.

To see the effect of slope ground, the above simulations are re-run with a ground slope of $\alpha = 7^o$. Due to the large swing velocity between 1 to 6 seconds, the gravity torque T_g changes quite rapidly. Also, its magnitude is so large that it dominates model uncertainties–a perfect example where model uncertainties are mainly due to uncertain nonlinearities. Traditionally, in such a case, adaptive control will normally perform poorly and even become unstable sometimes. However, the tracking errors shown in Fig. 6 reveal that the proposed ARC still has an excellent velocity tracking capability and achieves a better performance than DRC in spite of the unavoidable appearance of large uncertain nonlinearities. Overall, the proposed strategy can handle the variation of changing gravity load well.

5 Conclusions

The control issues associated with the swing motion, swing motors, and the dynamic interactions between the swing motion and swing motors of hydraulic excavators are considered in the paper. By treating the load flow rate as the control input, a novel ARC control strategy has been proposed to handle model uncertainties due to the unknown and time-varying swing inertia, large variations of hydraulic parame-

ters, the unknown leakage flows of the swing motors, and the fast changing and unknown swing gravity torque on a slope ground altogether at once. The unique contributions of the proposed work are thus as follows: (i) A novel backstepping ARC design has been presented for a class of nonlinear systems whose state equations cannot be linearly parametrized by a set of unknown parameters to address the control issues due to the unknown and time-varying inertia; (ii) Some of the particular control problems in the high performance swing motion control of hydraulic machines are identified and rigorous mathematical formulation is presented; (iii) A particular ARC controller suitable for the studied application is presented, which integrates several desirable ARC structures such as the desired compensation ARC and the discontinuous projection based ARC. Simple yet theoretically rigorous specific robust control terms suitable for the application are constructed; and (iv) On-line desired velocity trajectory generation with acceleration limit is proposed for achieving a smooth acceleration/deceleration and pressure limiting. Trajectory initialization is also introduced to reduce transient response. Simulation results showed that the proposed strategy can deliver the expected swing velocity tracking with a smooth acceleration and deceleration while keeping working pressures of swing motors below the line relief pressure. The paper thus serves as a stepping stone in the development of high performance control algorithms for future hydraulic machines.

References

[1] H. E. Merritt, *Hydraulic control systems.* New York: Wiley, 1967.

[2] T. C. Tsao and M. Tomizuka, "Robust adaptive and repetitive digital control and application to hydraulic servo for noncircular machining," *ASME J. Dynamic Systems, Measurement, and Control*, vol. 116, pp. 24–32, 1994.

[3] P. M. FitzSimons and J. J. Palazzolo, "Part i: Modeling of a one-degree-of-freedom active hydraulic mount; part ii: Control," *ASME J. Dynamic Systems, Measurement, and Control*, vol. 118, no. 4, pp. 439–448, 1996.

[4] A. R. Plummer and N. D. Vaughan, "Robust adaptive control for hydraulic servosystems," *ASME J. Dynamic System, Measurement and Control*, vol. 118, pp. 237–244, 1996.

[5] C. E. Jeronymo and T. Muto, "Application of unified predictive control (upc) for an electro-hydraulic servo system," *JSME Int. J., Series C*, vol. 38, no. 4, pp. 727–734, 1995.

[6] J. E. Bobrow and K. Lum, "Adaptive, high bandwidth control of a hydraulic actuator," *ASME J. Dynamic Systems, Measurement, and Control*, vol. 118, pp. 714–720, 1996.

[7] R. Vossoughi and M. Donath, "Dynamic feedback linearization for electro-hydraulically actuated control systems," *ASME J. Dynamic Systems, Measurement, and Control*, vol. 117, no. 4, pp. 468–477, 1995.

[8] L. D. Re and A. Isidori, "Performance enhancement of nonlinear drives by feedback linearization of linear-bilinear cascade models," *IEEE Trans. on Control Systems Technology*, vol. 3, no. 3, pp. 299–308, 1995.

[9] A. Alleyne and J. K. Hedrick, "Nonlinear adaptive control of active suspension," *IEEE Trans. on Control Systems Technology*, vol. 3, no. 1, pp. 94–101, 1995.

[10] B. Yao, G. T. C. Chiu, and J. T. Reedy, "Nonlinear adaptive robust control of one-dof electro-hydraulic servo systems," in *ASME International Mechanical Engineering Congress and Exposition (IMECE'97), FPST-Vol.4*, (Dallas), pp. 191–197, 1997.

[11] B. Yao and M. Tomizuka, "Smooth robust adaptive sliding mode control of robot manipulators with guaranteed transient performance," in *Proc. of American Control Conference*, pp. 1176–1180, 1994. The full paper appeared in *ASME Journal of Dynamic Systems, Measurement and Control*, Vol. 118, No.4, pp764-775, 1996.

[12] B. Yao and M. Tomizuka, "Adaptive robust control of siso nonlinear systems in a semi-strict feedback form," *Automatica*, vol. 33, no. 5, pp. 893–900, 1997. (Part of the paper appeared in Proc. of 1995 American Control Conference, pp2500-2505).

[13] B. Yao, "High performance adaptive robust control of nonlinear systems: a general framework and new schemes," in *Proc. of IEEE Conference on Decision and Control*, pp. 2489–2494, 1997.

[14] A. J. Koivo, M. Thoma, E. Kocaoglan, and J. Andrade-Cetto, "Modeling and control of excavator dynamics during digging operation," *J. of Aerospace Engineering*, no. 1, pp. 10–18, 1996.

[15] D. A. Bradley and D. W. Seward, "The development, control and operation of an autonomous robotic excavator," *J. of Intelligent and Robotic Systems*, vol. 21, pp. 73–97, 1998.

[16] J. V. Medanic and M. Z. Yuan, "Robust multivariable nonlinear control of a two link excavator: part i," in *Proc. 36th IEEE Conf. on Decision and Control*, pp. 4231–4236, 1997.

[17] M. Krstic, I. Kanellakopoulos, and P. V. Kokotovic, *Nonlinear and adaptive control design*. New York: Wiley, 1995.

[18] B. Yao and M. Tomizuka, "Comparative experiments of robust and adaptive control with new robust adaptive controllers for robot manipulators," in *Proc. of IEEE Conf. on Decision and Control*, pp. 1290–1295, 1994.

[19] B. Yao, "Hydraulic excavator (hex) swing control strategy." Project Report, Aug. 1997.

[20] N. Sadegh and R. Horowitz, "Stability and robustness analysis of a class of adaptive controllers for robot manipulators," *Int. J. Robotic Research*, vol. 9, no. 3, pp. 74–92, 1990.

[21] B. Yao and M. Tomizuka, "Robust desired compensation adaptive control of robot manipulators with guaranteed transient performance," in *Proc. of IEEE Conf. on Robotics and Automation*, pp. 1830–1836, 1994.

[22] S. Sastry and M. Bodson, *Adaptive Control: Stability, Convergence and Robustness*. Englewood Cliffs, NJ 07632, USA: Prentice Hall, Inc., 1989.

Appendix

P1: Proof of Lemma 1

Noting the first equation of (9), the derivative of (13) is

$$\begin{aligned}\dot{V}_1 &= e_\omega(I\dot{e}_\omega + \tfrac{1}{2}\dot{I}e_\omega) = e_\omega(D_{mp}P_L - \dot{I}\omega - \hat{T}_{loss} + \beta_2 - I\dot{\omega}_d + \tfrac{1}{2}\dot{I}e_\omega) \\ &= e_\omega(D_{mp}e_p + D_{mp}P_{Ld} - \dot{I}\omega_d - \hat{T}_{loss} + \beta_2 - I\dot{\omega}_d - \tfrac{1}{2}\dot{I}e_\omega) \\ &= e_\omega D_{mp}e_p + \dot{V}_1 \mid_{e_p=0}\end{aligned} \tag{29}$$

where $\dot{V}_1 \mid_{e_p=0}$ represents $\dot{V}_1$ when $e_p = 0$ and is given by

$$\dot{V}_1 \mid_{e_p=0} = e_\omega(D_{mp}P_{Ld} - \dot{I}\omega_d - \hat{T}_{loss} + \beta_2 - I\dot{\omega}_d - \tfrac{1}{2}\dot{I}e_\omega) \tag{30}$$

Substituting (14) into (30) and noting (16), we have

$$\dot{V}_1 \mid_{e_p=0} \quad = -(k_\omega I_c + \tfrac{1}{2}\dot{I})e_\omega^2 + e_\omega \left[D_{mp} P_{Lds} - \phi_{\omega 1}\tilde{\beta}_1 - \tilde{\beta}_2 \right] \tag{31}$$

which leads to (17) by noting condition i of (15), and (18) by noting condition ii of (15). □

P2: Proof of Remark 2

Due to the use of projection mapping in the parameter adaptation law (23), $\hat{\beta}$ is bounded by $\beta_{min} \le \hat{\beta} \le \beta_{max}$ [11, 13]. Thus, $\tilde{\beta}$ is bounded by $|\tilde{\beta}| \le \beta_M$ where $\beta_M = \beta_{max} - \beta_{min}$. Then,

$$\begin{aligned} e_\omega \left[D_{mp} P_{Lds} - \phi_{\omega 1}\tilde{\beta}_1 - \tilde{\beta}_2 \right] &\le -C_{s1} e_\omega^4 + |e_\omega|(|\phi_{\omega 1}|\beta_{M1} + \beta_{M2}) \\ &\le \tfrac{3}{4(4C_{s1})^{\frac{1}{3}}} \left(|\phi_{\omega 1}|\beta_{M1} + \beta_{M2}\right)^{\frac{4}{3}} \end{aligned} \tag{32}$$

in which the inequality $|xy| \le \frac{1}{p}|x|^p + \frac{1}{q}|y|^q, \quad \forall x, y \in R, \quad p > 0, q > 0$ with $\frac{1}{p} + \frac{1}{q} = 1$ has been used. Since $\phi_{\omega 1}$ defined by (16) depends on the desired trajectory only and is bounded, it is thus clear that condition i of (15) is satisfied with a larger C_{s1} corresponding to a smaller ε_ω. Condition ii of (15) is obviously satisfied. □

P3: Proof of Theorem 1

Noting (29), (9), and (11), the derivative of V given by (21) is

$$\begin{aligned} \dot{V} &= \dot{V}_1 \mid_{e_p=0} + e_\omega D_{mp} e_p + w_p e_p [I\dot{e}_p + \tfrac{1}{2}\dot{I}e_p] \\ &= \dot{V}_1 \mid_{e_p=0} + w_p e_p \left\{ \tfrac{1}{w_p} D_{mp} e_\omega + I \left[\beta_3 (Q_L - D_m\omega - \hat{Q}_{loss}) + \beta_4 - \dot{P}_{Ld} \right] + \tfrac{1}{2}\dot{I}e_p \right\} \\ &= \dot{V}_1 \mid_{e_p=0} + w_p e_p \left\{ \tfrac{1}{w_p} D_{mp} e_\omega + (I_c\beta_3 + I_{c\beta}\beta_5)(Q_L - D_m\omega - \hat{Q}_{loss}) + I_c\beta_4 + I_{c\beta}\beta_6 - I\dot{P}_{Ld} + \tfrac{1}{2}\dot{I}e_p \right\} \end{aligned} \tag{33}$$

From (14) and (9),

$$\begin{aligned} I\dot{P}_{Ld} &= I \left\{ \tfrac{\partial P_{Ld}}{\partial \omega}\dot{\omega} + \tfrac{\partial P_{Ld}}{\partial t} + \tfrac{\partial P_{Ld}}{\partial \hat{\beta}_1}\dot{\hat{\beta}}_1 + \tfrac{\partial P_{Ld}}{\partial \hat{\beta}_2}\dot{\hat{\beta}}_2 \right\} \\ &= \tfrac{\partial P_{Ld}}{\partial \omega}(D_{mp}P_L - \dot{I}\omega - \hat{T}_{loss} + \beta_2) + I\tfrac{\partial P_{Ld}}{\partial t} + I\tfrac{\partial P_{Ld}}{\partial \hat{\beta}_1}\dot{\hat{\beta}}_1 + I\tfrac{\partial P_{Ld}}{\partial \hat{\beta}_2}\dot{\hat{\beta}}_2 \\ &= \widehat{I\dot{P}_{Ld}} + \tfrac{\partial P_{Ld}}{\partial \omega}(\tilde{\dot{I}}\omega - \tilde{\beta}_2) - \tilde{I}\tfrac{\partial P_{Ld}}{\partial t} + I\tfrac{\partial P_{Ld}}{\partial \hat{\beta}_1}\dot{\hat{\beta}}_1 + I\tfrac{\partial P_{Ld}}{\partial \hat{\beta}_2}\dot{\hat{\beta}}_2 \end{aligned} \tag{34}$$

where $\widehat{I\dot{P}_{Ld}}$ represents the calculable part of $I\dot{P}_{Ld}$ and is defined in (22), and the rest terms represent the incalculable part due to parametric uncertainties.

Note that $\tilde{\dot{I}} = \dot{I}_{c\beta}\tilde{\beta}_1$ and $\tilde{I} = I_{c\beta}\tilde{\beta}_1$. By substituting (24) and (34) into (33) and grouping terms according to the terms defined in (22), we have

$$\begin{aligned}\dot{V} &= \dot{V}_1 \mid_{e_p=0} + w_p e_p \Big\{ (I_c\beta_3 + I_{c\beta}\beta_5)Q_{Lds} + (I_c\hat{\beta}_3 + I_{c\beta}\hat{\beta}_5)(Q_{Lda} - D_m\omega - \hat{Q}_{loss}) \\ &\quad -(I_c\tilde{\beta}_3 + I_{c\beta}\tilde{\beta}_5)(Q_{Lda} - D_m\omega - \hat{Q}_{loss}) - \alpha_{2c} - I_c\tilde{\beta}_4 - I_{c\beta}\tilde{\beta}_6 \\ &\quad -\tfrac{\partial P_{Ld}}{\partial\omega}(\tilde{\dot{I}}\omega - \tilde{\beta}_2) + \tilde{I}\tfrac{\partial P_{Ld}}{\partial t} - I\tfrac{\partial P_{Ld}}{\partial\hat{\beta}_1}\dot{\hat{\beta}}_1 - I\tfrac{\partial P_{Ld}}{\partial\hat{\beta}_2}\dot{\hat{\beta}}_2 + \tfrac{1}{2}\dot{I}e_p \Big\} \\ &= \dot{V}_1 \mid_{e_p=0} -(k_pI_c - \tfrac{1}{2}\dot{I})w_pe_p^2 + w_pe_p\left\{ I\beta_3 Q_{Lds} - \phi_p^T\tilde{\beta} - I\tfrac{\partial P_{Ld}}{\partial\hat{\beta}_1}\dot{\hat{\beta}}_1 - I\tfrac{\partial P_{Ld}}{\partial\hat{\beta}_2}\dot{\hat{\beta}}_2 \right\}\end{aligned} \tag{35}$$

Noting conditions i of (15) and (25) respectively, from (31) and (35), we have

$$\begin{aligned}\dot{V} &\le \dot{V}_1 \mid_{e_p=0} + \tfrac{1}{2}k_\omega I_c e_\omega^2 - \tfrac{1}{2}(k_pI_c - \dot{I})w_pe_p^2 + \varepsilon_p \\ &\le -\tfrac{1}{2}(k_\omega I_c + \dot{I})e_\omega^2 + \varepsilon_\omega - \tfrac{1}{2}(k_pI_c - \dot{I})w_pe_p^2 + \varepsilon_p \\ &\le -\lambda_V V + \varepsilon_V\end{aligned} \tag{36}$$

which leads to (26). Thus Result a) of Theorem 1 is proved.

To prove result b) of Theorem 1, substitute (31) into (35):

$$\begin{aligned}\dot{V} &= -(k_\omega I_c + \tfrac{1}{2}\dot{I})e_\omega^2 + e_\omega D_{mp}P_{Lds} - e_\omega\phi_{\omega 1}\tilde{\beta}_1 - e_\omega\tilde{\beta}_2 \\ &\quad -(k_pI_c - \tfrac{1}{2}\dot{I})w_pe_p^2 + w_pe_p\left\{ I\beta_3 Q_{Lds} - I\tfrac{\partial P_{Ld}}{\partial\hat{\beta}_1}\dot{\hat{\beta}}_1 - I\tfrac{\partial P_{Ld}}{\partial\hat{\beta}_2}\dot{\hat{\beta}}_2 \right\} - w_pe_p\phi_p^T\tilde{\beta} \\ &= -(k_\omega I_c + \tfrac{1}{2}\dot{I})e_\omega^2 - \tau_\beta^T\tilde{\beta} + e_\omega D_{mp}P_{Lds} - (k_pI_c - \tfrac{1}{2}\dot{I})w_pe_p^2 + w_pe_p\left\{ I\beta_3 Q_{Lds} - I\tfrac{\partial P_{Ld}}{\partial\hat{\beta}_1}\dot{\hat{\beta}}_1 - I\tfrac{\partial P_{Ld}}{\partial\hat{\beta}_2}\dot{\hat{\beta}}_2 \right\}\end{aligned} \tag{37}$$

where τ_β is defined in (22). Noting conditions ii of (15) and (25) respectively, (37) leads to

$$\dot{V} \le -\tfrac{1}{2}(k_\omega I_c + \dot{I})e_\omega^2 - \tfrac{1}{2}(k_pI_c - \dot{I})w_pe_p^2 - \tau_\beta^T\tilde{\beta} \tag{38}$$

Following the same proof as in [11, 13], it can be shown that (38) and the adaptation law (23) lead to asymptotic output tracking in the presence of constant parametric uncertainties, i.e., $e_\omega \longrightarrow 0$ as $t \longrightarrow \infty$ when β is constant. This proves Result b) of Theorem 1.

The following is to prove c) of Theorem 1. If (27) is true, then, $e_\omega(0) = 0$, and

$$P_L(0) = \tfrac{1}{D_{mp}}\left[\hat{I}\dot{\omega}_d(0) + \hat{\dot{I}}\omega + \hat{T}_{loss} - \hat{\beta}_2 \right] \mid_{t=0} \tag{39}$$

Thus, from (14) and (20), it is evident that $P_{Lda}(0) = P_L(0)$ and $P_{Lds}(0) = 0$. Therefore, $e_p(0) = P_L(0) - P_{Ld}(0) = 0$, and thus $V(0) = 0$. □

P4: Proof of Remark 5

From (23) and the property of projection mapping [11, 13], $|\dot{\hat{\beta}}_1| \leq |\gamma_1\tau_{\beta 1}|$ and $|\dot{\hat{\beta}}_2| \leq |\gamma_2\tau_{\beta 2}|$. Thus, noting (22), we have

$$\begin{aligned} e_p \left\{ -I\tfrac{\partial P_{Ld}}{\partial \hat{\beta}_1}\dot{\hat{\beta}}_1 - I\tfrac{\partial P_{Ld}}{\partial \hat{\beta}_2}\dot{\hat{\beta}}_2 \right\} &\leq I|e_p\tfrac{\partial P_{Ld}}{\partial \hat{\beta}_1}||\gamma_1\tau_{\beta 1}| + I|e_p\tfrac{\partial P_{Ld}}{\partial \hat{\beta}_2}||\gamma_2\tau_{\beta 2}| \\ &\leq \gamma_1 I|\tfrac{\partial P_{Ld}}{\partial \hat{\beta}_1}|(|\phi_{\omega 1}||e_p||e_\omega| + |\phi_{p1}|w_p e_p^2) + \gamma_2 I|\tfrac{\partial P_{Ld}}{\partial \hat{\beta}_2}|(|e_p||e_\omega| + |\phi_{p2}|w_p e_p^2) \\ &\leq I(\gamma_1|\tfrac{\partial P_{Ld}}{\partial \hat{\beta}_1}||\phi_{\omega 1}| + \gamma_2|\tfrac{\partial P_{Ld}}{\partial \hat{\beta}_2}|)|e_p||e_\omega| + I(\gamma_1|\tfrac{\partial P_{Ld}}{\partial \hat{\beta}_1}||\phi_{p1}| + \gamma_2|\tfrac{\partial P_{Ld}}{\partial \hat{\beta}_2}||\phi_{p2}|)w_p e_p^2 \\ &\leq \tfrac{1}{2w_p}k_\omega I_c e_\omega^2 + \left[\tfrac{1}{2k_\omega I_c}I^2(\gamma_1|\tfrac{\partial P_{Ld}}{\partial \hat{\beta}_1}||\phi_{\omega 1}| + \gamma_2|\tfrac{\partial P_{Ld}}{\partial \hat{\beta}_2}|)^2 + I(\gamma_1|\tfrac{\partial P_{Ld}}{\partial \hat{\beta}_1}||\phi_{p1}| + \gamma_2|\tfrac{\partial P_{Ld}}{\partial \hat{\beta}_2}||\phi_{p2}|)\right] w_p e_p^2 \end{aligned} \tag{40}$$

Since $|\tilde{\beta}| \leq \beta_M$,

$$w_p e_p \phi_p^T \tilde{\beta} \leq w_p|\phi_p|^T\beta_M|e_p| \leq \varepsilon_p + \tfrac{w_p^2}{4\varepsilon_p}(|\phi_p|^T\beta_M)^2 e_p^2 \tag{41}$$

Based on (40) and (41), by simple comparisons, it can be easily checked out that the two conditions of (25) are satisfied by Q_{Lds} given by (28). □

Figure 1: Overall Controller Structure

Figure 2: Desired Load Pressure for Velocity Tracking Control

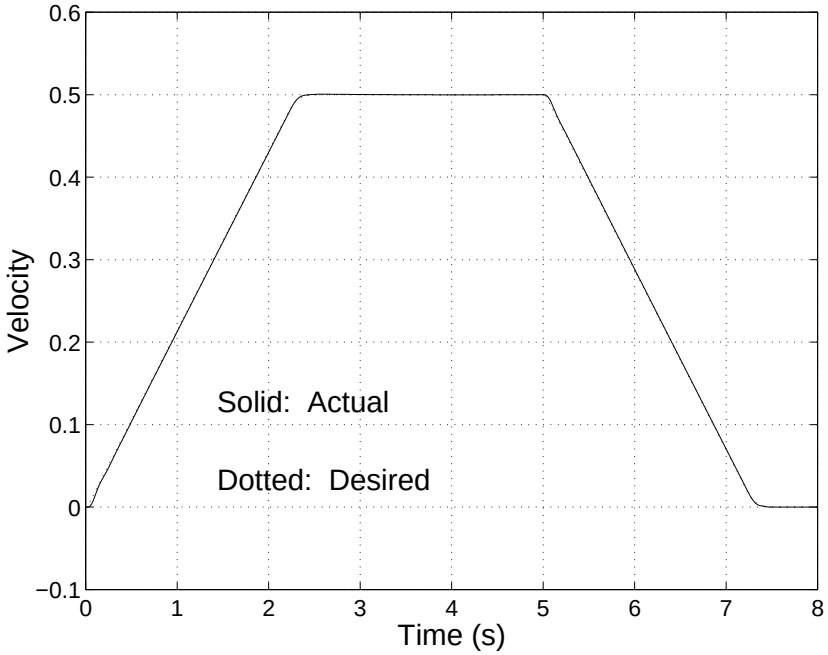

Figure 3: Swing Velocity Tracking On A Flat Ground

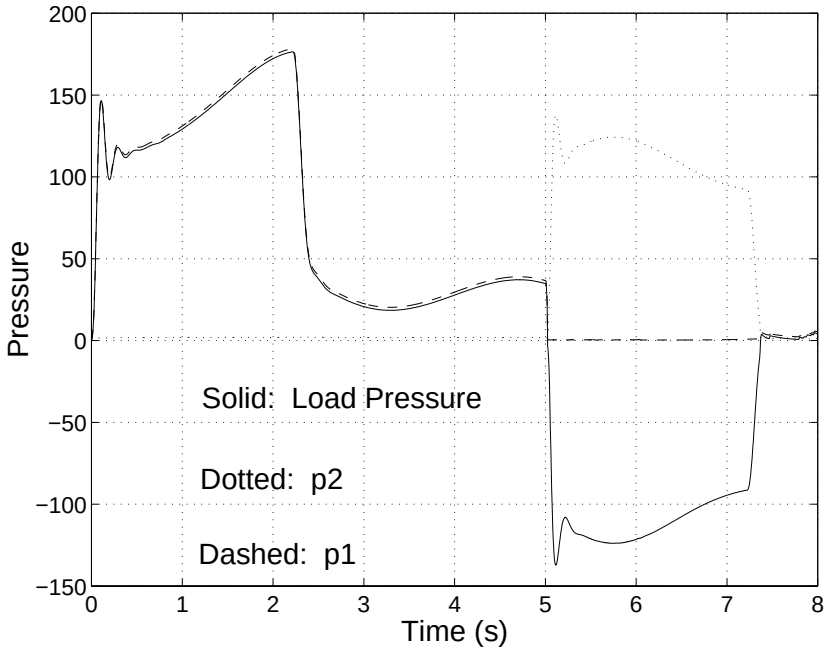

Figure 4: Working Pressures of Swing Motors

Figure 5: Velocity Tracking Error On An Even Ground

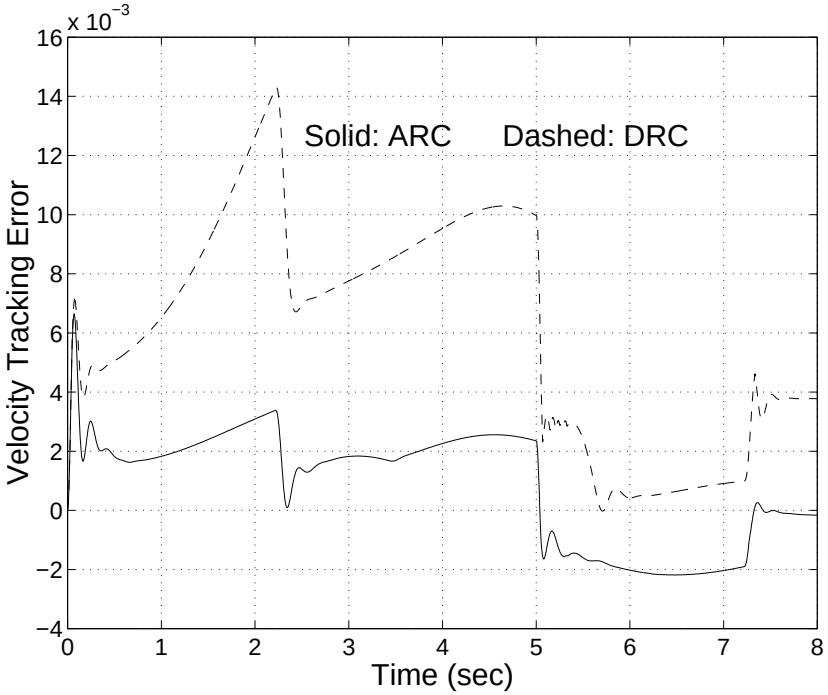

Figure 6: Velocity Tracking Error On A Slope Ground ($\alpha = 7^o$)